Journal of Power Sources 195 (2010) 1122–1129

Contents lists available at ScienceDirect

Journal of Power Sources

journal homepage: www.elsevier.com/locate/jpowsour

Experimental study on the two phase flow behavior in PEM fuel cell parallel channels with porous media inserts

Jixin Chen*,[1]

Mechanical and Aerospace Engineering, University of California, Irvine, Irvine, CA 92697-3975, USA

ARTICLE INFO

Article history:
Received 8 July 2009
Received in revised form 1 September 2009
Accepted 2 September 2009
Available online 11 September 2009

Keywords:
PEM fuel cell
Porous media
Two phase flow
Pressure drop
Flow mal-distribution
Water hold-up

ABSTRACT

In this study, the air–water two phase flow behavior in PEM fuel cell parallel channels with porous media inserts was experimentally investigated using a self-designed and manufactured transparent assembly. The visualization images of the two phase flow in channels with porous media inserts were presented and three patterns were summarized. Compared with the traditional hollow channel design, the novel configuration featured less severe two phase flow mal-distribution and self-adjustment to water amount in channels, although a higher pressure drop was introduced due to the porous media inserts. The dominant frequency of pressure drop signal was found to be a diagnostic tool for water behavior in channels. The novel flow channel design with porous media inserts may become a solution to the water management problem in PEM fuel cells.

1. Introduction

The Proton Exchange Membrane (PEM) fuel cell has been regarded as an ideal power source for a variety of applications due to its significant advantages, *i.e.*, high efficiency, low emission, silence and simplicity [1]. The water management is currently considered as one of the crucial issues to be fully understood and optimized before a successful commercialization of PEM fuel cells, since sufficient amount of water is necessary for maintaining the membrane ion conductivity whereas excess water, or water flooding, may block the porous electrodes and flow channels, reducing the reactant mass transfer to catalytic sites [2–5]. Considering the low operating temperature (<85 °C) and pressure (<4 bar), the phenomena of two phase flows are unavoidable. The two phase flow problem in PEM fuel cell consists of liquid water generation and transport in catalyst layer/gas diffusion layer, and two phase transport in flow channels. Most of the modeling researches focused on the first two problems [6–9], whereas only a few on the two phase flow in flow channels [10,11]. Also, most early models have simplified the two phase channel flow, *i.e.*, they considered only a single phase flow [12,13]. The significance of the two phase flow behavior in fuel cell flow channels has been gradually realized and recently many relevant numerical and experimental studies were conducted [14–17]. Specifically, Zhang et al. [18,19] conducted systematic ex situ studies on the two phase flow patterns and flow distributions in parallel channels, where they mainly concerned the mal-distribution and flow hysteresis phenomenon. Basu et al. [20] recently reported a complete two phase flow model that was validated against their experimental data. Considering the gas diffusion layer (GDL) intrusion into channels, their model explored the two phase flow mal-distribution in parallel channels in detail.

The analogy between mini-channels and random porous media in terms of the two phase flow behavior has been reported by many researchers [21–24]. Particularly for PEM fuel cell channel flow, Wang et al. [11] proposed a model to study the channel flow and theoretically obtained the solutions for two phase flow in fuel cell channels. It was also proposed for the first time that channels can generally be treated as porous media with or without porous inserts [11]. Motivated by the homogeneity between PEM fuel cell flow channels with and without porous media inserts, the author experimentally investigated the two phase flow behavior in the channels with porous inserts in this study. The findings suggest that inserting porous media into flow channels may become a novel solution to the water management problem. This is a completely new design for the flow channel, which has changed the traditional understanding that flow channel has to be hollow.

Carbon paper/cloth, as a common porous media, has been widely applied as the GDL material. Many modeling studies were performed to investigate the two phase flow in the porous GDL or electrode. Sinha and Wang [25] developed a pore-network model

* Tel.: +1 949 824 0701; fax: +1 949 824 8585.
E-mail address: jixinc@uci.edu.
[1] Present address: Mechanical Engineering, University of Michigan, Ann Arbor, MI 48109, USA.

0378-7753/$ – see front matter © 2009 Elsevier B.V. All rights reserved.
doi:10.1016/j.jpowsour.2009.09.004

to study the liquid water movement and flooding in GDL. They found that capillary forces control liquid water transport in the GDL. Tabe et al. [26] conducted numerical simulations using the lattice Boltzmann method (LBM) to elucidate the dynamic behavior of condensed water in GDL. They suggested the possibility of controlling two phase distribution to the catalyst layer by gradient wettability design of the porous separator. Recently a general three-dimensional model to investigate multiphase flows and species transport in the GDL has been developed by Wang [27]. Experimental studies about the two phase flow in GDL mainly focused on the water transport/removal using ex situ characterization. Benziger et al. [28] reported their measurements of the pressure required to push water through different layers of gas diffusion media. They suggested that the size of the pores resulted in different water transport behaviors. Gao et al. [29] used confocal microscopy technique to capture the real-time transport of water in GDL. They found that water followed distinct flow paths spanning several pores to form a column flow during the transport. Jiao et al. [30] studied the effect of GDL thickness on the liquid water removal characteristics and also presented the visualization of water removal.

It should be noted that although many researches have been conducted on the two phase flow in porous media as GDL, there is little found in the open literature concerning the effects of porous media inserts into the fuel cell flow channels due to its novelty. In this study, the author chose carbon foam as the porous media to fill the channels. Compared with carbon paper/cloth, carbon foams have much more better mechanical strength so that it can be precisely machined to micro-sized bar to fit the fuel cell channels. Also, the pore size can be determined by its product specification pores per inch (PPI). A wide range of structural properties and permeabilities for multi-applications can be obtained. Finally, commercial carbon foams are not processed by PTFE as carbon paper/cloth, so that we may examine the pure effects of porous media inserts without influences from hydrophobic/hydrophilic property. Usage of porous foams has been found in some energy relevant researches. Arisetty et al. [31] incorporated metal foams as the flow field in direct methanol fuel cell and investigated the influences of pore size and density on the cell performance. Jang et al. [32] replaced traditional lead alloys by graphite foams for the development of lightweight lead acid batteries. Yang et al. [33] prepared nickel foam cathodes for an aluminum–hydrogen peroxide fuel cell and studied the electrochemical performance and stability of the cathode. As reviewed by Ströbel et al. [34], Ni foam with carbon nanotubes pressed in has been considered as a good candidate of hydrogen storage material. However, the application of porous foams in PEM fuel cell, particularly its flow channels, has not been found in open literature. This study, therefore, may become the first attempt to apply such material in PEM fuel cell technology. The objective is to systematically investigate the effects of porous media inserts on the two phase flow in the regular parallel fuel cell flow channels. Two phase flow in hollow fuel cell flow channels without porous inserts has been studied [18,19], which provide a good comparison reference.

2. Experimental

In this work, an assembly similar to the transparent PEM fuel cell [17] was self-designed and precisely manufactured using CNC machine. It consists of an end plate with two parallel micro-channels built on, a transparent plastic plate for visualization and a window plate to apply even compression to the whole assembly. Necessary O-rings were placed on site to avoid leakage. The width of the channel is 1.5 mm and the depth is 1.2 mm; consistent with typical fuel cell designs. The effective length of the channel is 40 mm, with an entrance region to stabilize the air flow. Since the

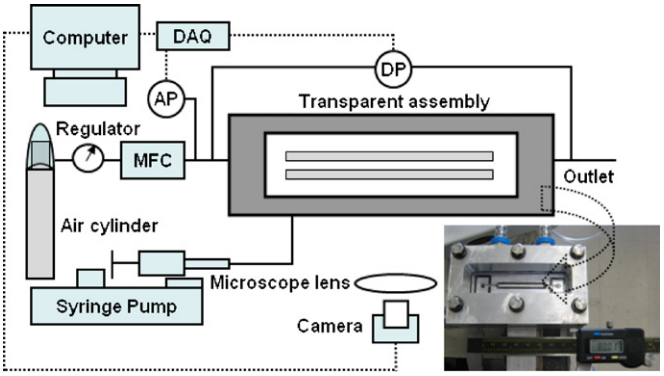

Fig. 1. Schematic of the experimental setup.

core frictional pressure drop in the developing (entrance) region of the channel is non-linear and unstable [35], the pressure drop measurement was only performed on the effective length (40 mm) of the channel. Pressure measurement ports were precisely drilled at two ends of the channels. The experimental setup is schematically shown in Fig. 1, with a photo of the transparent assembly attached. The air flow rate was controlled by a mass flow controller in the fuel cell test system from Scribner Associate, Inc. The absolute pressure at the air flow inlet and the differential pressure across the whole channel were measured by Omega PX219 and Setra 230 series transducers, respectively. Measurement data from the transducers were real-time displayed and recorded using self-developed LabVIEW programs. A CCD camera was attached to the microscope to capture the real-time flow video. A three-dimensional workbench was designed to hold the transparent assembly and perform the micro-movement. During the experiments, the workbench could be readily adjusted so that the view field from the camera and microscope achieved the best resolution. Liquid water was injected into the channels using a syringe pump, which has four syringe slots but only two were used, so that the injection rate was accurately controlled. The injection ports were drilled at one end of each channel and at another end corresponding ports were arranged to collect the water draining out from each channel, which was then weighed in a beaker and by a balance. The water injection rate was set to 0.005, 0.01 and 0.03 ml min^{-1} as three cases, corresponding to liquid velocity in each channel (U_l) of 0.046, 0.093 and 0.278 m s^{-1}, respectively. This was an analogy to the real fuel cell operation given a normal current density of 0.6 A cm^{-2} and an effective MEA area of 4 cm^2. 0.01 ml min^{-1} was the base rate and other two simulated drying and flooding conditions in the channels, respectively. Meanwhile, air flow rate was varied from 0.01 to 0.8 l min^{-1}, corresponding to a stoichiometry ratio up to 10 in fuel cell operation, and a gas velocity in each channel (U_g) from 0.09 to 3.7 m s^{-1} (assuming there was no mal-distribution).

The porous media used in the experiments were from ERG Materials and Aerospace Corp. Duocel® carbon foams with a relative density (porosity) of 3% and pore size of 80 and 100 PPI were selected for the experimental tests. According to Ref. [36], the strut diameter d_f, pore size d_p and porosity ε can be related by:

$$\frac{d_f}{d_p} = 2\sqrt{\frac{1-\varepsilon}{3\pi}}\frac{1}{G}, \quad \text{where } G = 1 - e^{-(1-\varepsilon)/0.04}$$

Therefore, the actual pore size was calculated to be ~120 and ~100 μm, respectively. The average pore size of GDL in PEM fuel cell is usually ~30 μm, and porosity ~80%. The carbon foam in this study has different specifications for two reasons: first, too small pore may be unfavorable for visualization of water transport in porous media; second, considering there is no electrochemical reactions in gas channels and the homogeneity between hollow channel and

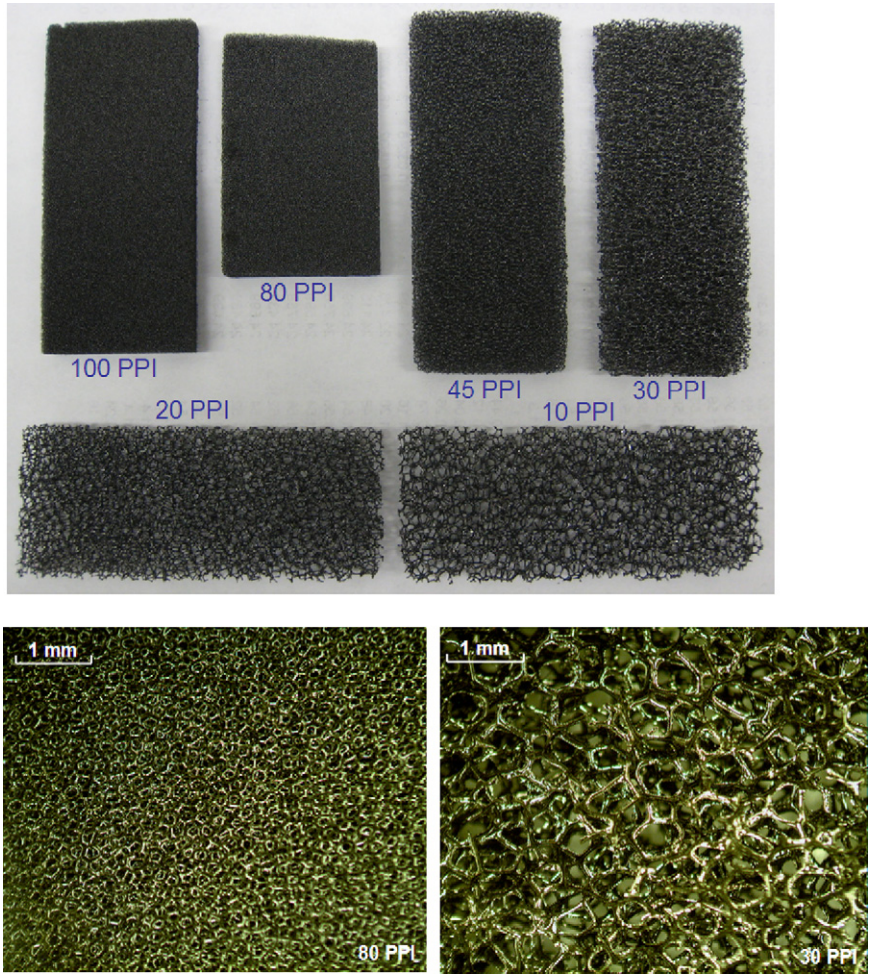

Fig. 2. Photos of the carbon foams used in this study.

porous media channel, high porosity becomes unnecessary. Fig. 2 shows the carbon foams with different pore sizes. Two representative microscopy images (80 and 30 PPI) are also presented. To accurately fit the channels, carbon foams were cut on the milling machine. Two carbon foam bars with the same size to the channels were prepared and carefully placed into the channels. As such slim carbon foam bars were very brittle, extreme care was taken to fill them into the channels.

3. Results and discussion

3.1. Two phase flow patterns in porous channels

In this section, the two phase flow patterns in the channels with porous media inserts are presented. Previous study of two phase flow in hollow micro-channels has clarified the general patterns [37]. Specifically for PEM fuel cell applications, the two phase patterns are principally droplet, film and slug flows [17,38]. In this study, however, porous media were filled into the channels, which produced different results.

Fig. 3 shows the images of the channel flow captured by the CCD camera. All the photos were taken after the system stabilized. To better illustrate the two phase flow behavior in the porous channel, schematic diagrams are also presented for each case. In Fig. 3(a), the air flow rate was 0.0566 l min^{-1}. The injected water was randomly distributed in some of the pores. The air flow passed through the channel via those hollow pores without water hold-up, meanwhile pushing the water in other pores. As water droplets in pores, they were moving to neighboring pores with overall directions being forward, upward and downward. Some of the water droplets were transporting within the pore network in the channel, whereas some were expelled eventually out of the channel by the air flow. Consequently, a portion of the injected water was hold within the porous media, about which a further discussion will be presented in Section 3.4. The water expelling was not continuous in this case, as represented by the solid line in Fig. 4, the pressure drop historical profile, since every peak indicated a removal of certain amount of water at the outlet. The relatively lower pressure drop between two peaks corresponded to the water movement within the porous channel but no removal out. The discontinuous water removal was attributed to the low air flow rate, which resulted in multi-direction and random movement of water in pores and failed to supply sufficient high pressure to expel the water out continuously, as the pressure needed to build-up to overcome the surface capillary energy before the hold-up water near the outlet can be removed out. In addition, the water hold-up in pores showed a group accumulation and movement effect, that is, in some regions the whole channel width was occupied from the top view whereas in other regions only a little occupied. An overall view therefore resembled the slug flow pattern in hollow micro-channel.

When air flow rate was increased to 0.2366 l min^{-1}, as illustrated in Fig. 3(b), the water films were formed at the two sides of the channel within the porous media. This is because the increased air flow moved the water in pores towards the side of the channel when the flow front touched the water. After the formation of

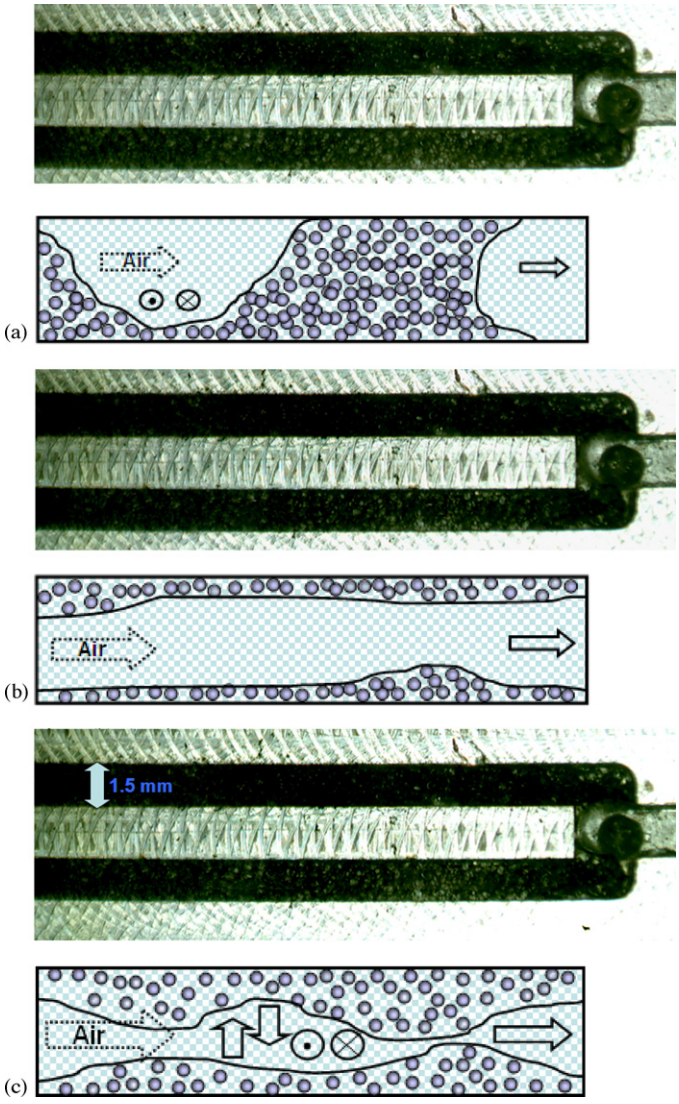

Fig. 3. Visualization image and schematic diagram of the two phase flow in porous channels at water injection rate of 0.01 ml min^{-1} and (a) air flow rate of 0.0566 l min^{-1}; (b) air flow rate of 0.2366 l min^{-1}; (c) air flow rate of 0.3266 l min^{-1}.

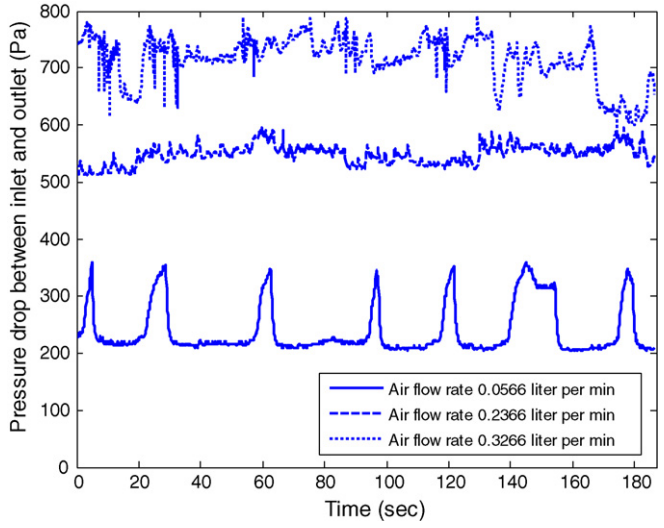

Fig. 4. Real-time pressure drop profiles at water injection rate of 0.01 ml min^{-1} and different air flow rates in Fig. 3.

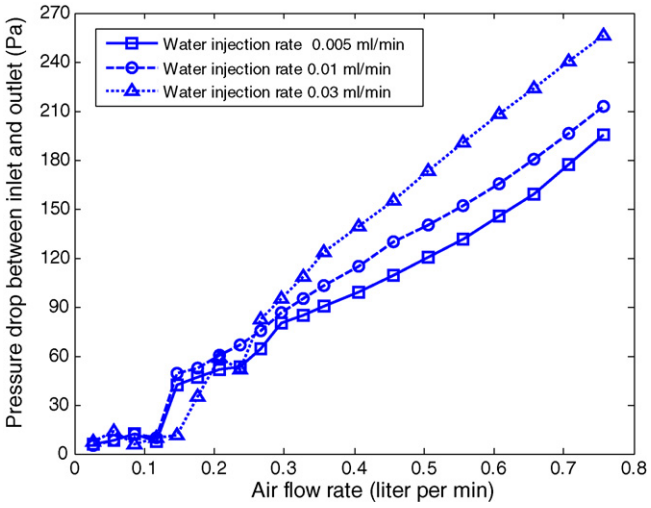

Fig. 5. Pressure drop profiles when the channels were hollow without porous inserts.

water film, it was pushed further towards the outlet. As a result, the water removal in this case was continuous, represented by the dashed line in Fig. 4.

Further increase of air flow rate to 0.3266 l min^{-1} resulted in a chaos water movement in porous media as shown in Fig. 3(c). Some of the water droplets in the water film were pushed back towards the center of the channel by the layers of air flow heading to the sides of the channel. They also moved in vertical directions both upwards and downwards. The water was removed continuously and quickly out of the channels; meanwhile, the water movement within the porous channels was intense. Therefore the dotted line in Fig. 4 presents a fairly irregular and coarse pressure drop, which was overall much higher than other two.

Since it may be the first time to study the two phase flow behavior in micro-channels with porous media inserts, these three patterns are named as intermittent flow, film flow and chaos flow, respectively.

3.2. Two phase flow pressure drop profiles

Fig. 5 shows the profiles of the two phase flow pressure drop across the whole channels when the channels were hollow, which was purposed for comparison with porous media channel. A common characteristic of these three curves is the pressure drop decrease followed by a sudden increase (around 0.1 l min^{-1} air flow rate). A similar phenomenon was reported in Refs. [18,39,40], reason being the two phase flow pattern transition from stratified flow in one channel and stagnant liquid in the other to stratified flows in both channels. There was apparent flow mal-distribution before such transition when one channel held stagnant liquid, and the mal-distribution immediately and greatly reduced after the transition when both channels presented stratified flows. The observed negative slope between pressure drop and air flow rate was closely linked with the flow mal-distribution change. As the air flow rate further increased after 0.2 l min^{-1}, the flow pattern turned out to be slug or stratified flow in both channels. The pressure drop did not see abrupt changes in this regime.

Fig. 6 plots the pressure drops against different air flow rates when the porous media was inserted. The data were taken when the system was stable. Since water was injected at very low rates for all three cases, it usually took more than 30 min for the system to stabilize. Compared with Fig. 5, the two phase pressure drop was overall higher (about fourfold increase) due to the insert of porous media. Also, higher water injection rate/air flow rate resulted in a

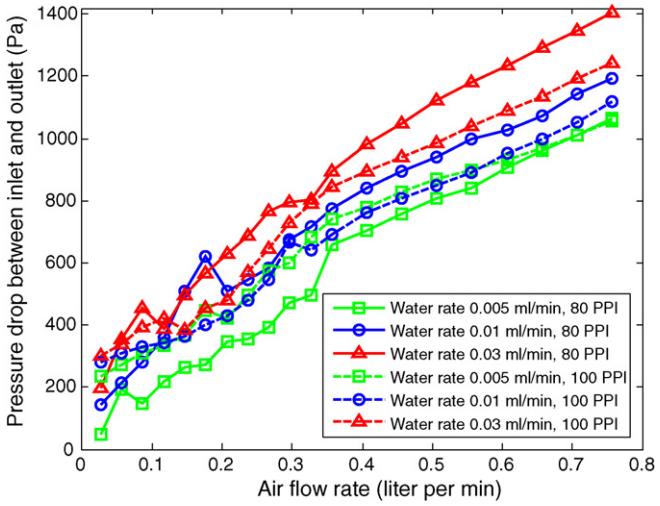

Fig. 6. Pressure drop profiles under different water injection rates and porous media pore sizes.

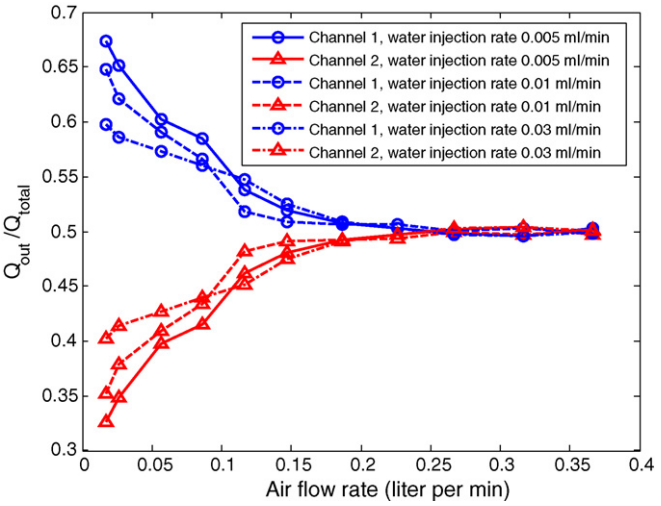

Fig. 7. The ratio of the collected water at one channel to the total from two channels when the channels were hollow without porous inserts.

relatively higher pressure drop. It should be noted that at the low air flow rate regime, negative slop between the pressure drop and air flow rate was still observed for all cases. For example, when the water injection rate was 0.03 ml min^{-1} and the pore size was 80 PPI, the two phase pressure drop decreased with an increase of air flow rate from 0.08 to 0.12 l min^{-1}. This negative flow resistance phenomenon may be also explained by the flow pattern transform, from intermittent flow to film flow as defined in Section 3.1. This finding indicates that inserting porous media into the micro-flow channels retains the negative flow resistance at low air flow rate, which confirms the homogeneity between hollow channel and porous channel. A careful inspection into Fig. 6 reveals an unusual pressure drop curve among others, *i.e.*, when the water injection rate was 0.005 ml min^{-1} and the pore size was 100 PPI; the pressure drop was very close to the cases with water injection rate of 0.01 ml min^{-1} (the blue lines). Also, it was apparently higher than the case with the same water injection rate but larger pore size (the solid green line), whereas for other cases larger pore size corresponded to higher pressure drop (the solid lines higher than the dashed lines). This phenomenon may be attributed to the water hold-up capacity of the porous media in channel. At relatively lower water injection rate (0.005 ml min^{-1}) and for smaller pore size carbon foam (100 PPI), a great amount of liquid water was hold in numerous pores instead of flowing out with the air, thereby increasing the two phase pressure drop across the channels. The water hold-up characteristic of the 100 PPI carbon foam predominated when the water injection rate was low. As the air flow rate increased to 0.65 l min^{-1} and further, much less water could be trapped in the porous media even for the 100 PPI foam, therefore such relatively higher pressure drop turned back (the dashed green line becomes lower than the solid green line, which is the normal trend). The pressure drop profiles at higher air flow rate show better linearity. A further discussion on the water hold-up of porous media will be presented in Section 3.4.

3.3. Two phase flow mal-distribution

The flow mal-distribution has been under study for decades. Back to twenty years ago, the mal-distribution in heat exchangers was summarized by Kitto and Robertson [41], who also suggested for the first time that the problem would be more serious and complicated in the case of two phase flow such as in the evaporator. Fuel cell, as an electrochemical device, further adds the complexity to the two phase flow mal-distribution since the water is generated at various catalytic spots and at varied speeds. The water generation and transport is difficult to model accurately, although many approaches and results can be found in literature, as reviewed at the beginning. Ex situ approaches therefore become significant nowadays since it is favorable to figure out the physics under the simplified condition, *i.e.*, no accompanying reactions. In this study, the author quantified the two phase mal-distribution by the ratio of the out-flowing water collected at one channel to the total from both channels. In Figs. 7–9, Q_{out} is the amount of liquid water collected from either channel 1 or channel 2 for 1 h; and obviously $Q_{total} = Q_{out,1} + Q_{out,2}$. If there was no mal-distribution, the ratio Q_{out}/Q_{total} would be around 0.5. Some strategies were applied to minimize the system error in this experiment. Every time before the water injection/collection, the system was purged by high flow rate air for long enough time to make sure the remaining water in the system was removed. The fitting at the outlet was also removed to avoid droplet attachment at the inner surface. In addition, the air had been passing through a humidifier in the fuel cell test system before it entered the transparent assembly. The pre-humidified air can absorb/condense little water when it passed though the channels as the temperature in the manifolds and channels was uniform at room temperature.

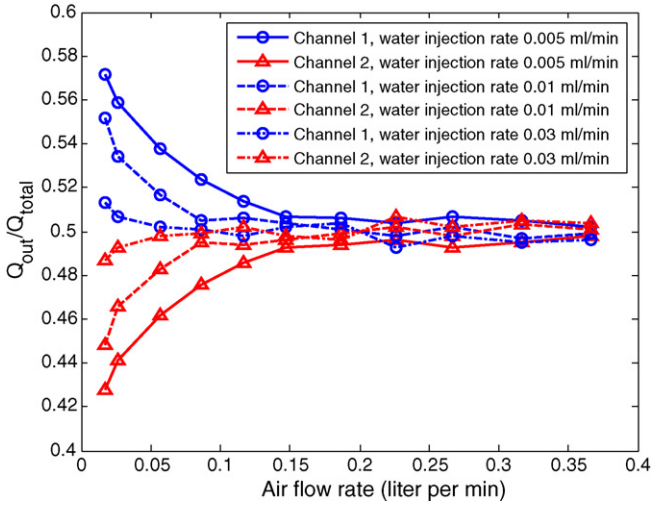

Fig. 8. The ratio of the collected water at one channel to the total from two channels for different air flow rates when the porous insert was 80 PPI carbon foam.

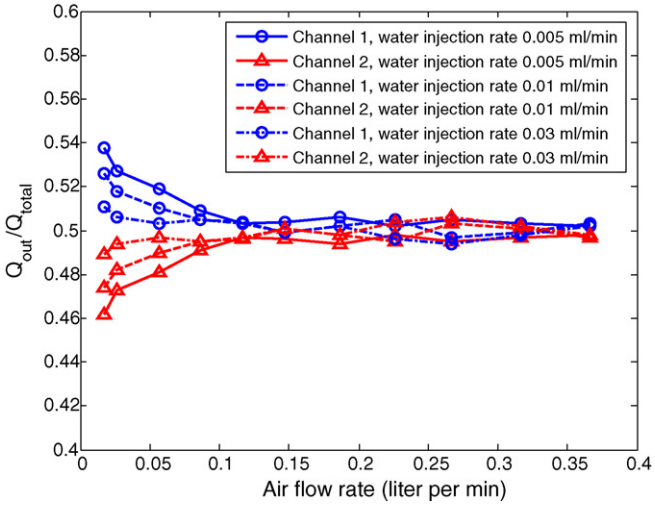

Fig. 9. The ratio of the collected water at one channel to the total from two channels for different air flow rates when the porous insert was 100 PPI carbon foam.

Fig. 7 gives the mal-distribution level when the channels were hollow without porous media inserts. At low air flow rates, the mal-distribution was severe (~0.65) for all three cases. Similar results were reported in Ref. [19]. For traditional hollow flow channel design, it is unavoidable to introduce mal-distribution due to the uneven flow resistance or water distribution. In this study, the injected water could hardly enter each channel with exactly identical amounts in spite of the same geometry for both channels. The resulted uneven flow resistance induced the two phase flow mal-distribution. As the flow tended to select the channel with less resistance, or more flow entered the channel with less resistance; the accumulation effect of the mal-distribution should be noted, until one channel being fully blocked. Then, a self-recovery or water removal might occur depending on the air flow rate and channel geometry. For an operating fuel cell, the uneven local current density may deteriorate the flow mal-distribution in channels, and the latter in turn influences the current output. One widely applied strategy is to supply the reactant flow at a fairly high stoichiometry; since at increased air flow rates, the mal-distribution was greatly reduced as shown in Fig. 7.

Fig. 8 presents the mal-distribution test results for porous media channels. As illustrated in Fig. 8, when the air flow rate was low, slight mal-distributions were observed (~0.56) compared with in Fig. 7. With increased air flow rate, the mal-distribution almost disappeared. When relatively smaller amount of water was injected ($0.005\ \mathrm{ml\ min^{-1}}$), the distribution in various pores of each channel tended to be more uneven as a random process, thereby producing a more severe mal-distribution. On the other hand, the cases with less water trapped, or increased air flow rates in porous media showed more even flow resistance for each channel and thus less severe mal-distribution. Overall, the flow mal-distribution had been reduced with the porous media inserts being introduced. It is speculated that the porous inserts reduced the mal-distribution by a random arrangement of liquid water droplets at various locations in the channel. The numerous tiny pores in channels provided the ease for achieving such random arrangement. As the water formed numerous tiny droplets (diameter ~100 μm) in the channel pore network, the uneven water distribution or flow resistance was greatly reduced. Fig. 9 presents the same plot with the carbon foam pore size of 100 PPI instead of 80 PPI. As clearly shown, the flow mal-distribution was further reduced compared with the previous case of 80 PPI foam in Fig. 8. The mal-distribution had been roughly eliminated; even at low air flow rate, it reached a maximum of ~0.54 only. This was due to a more random distribution of water droplets in smaller pores provided by the 100 PPI carbon foam. As a summary, porous media in flow channels may greatly reduce the flow mal-distribution; which shows a better effect as the pore size becomes smaller. This finding suggests a potential solution to the flow mal-distribution problem in fuel cell flow channels.

3.4. Water hold-up in porous media

Fig. 10 presents the water hold-up ratio in the porous media for different air flow rates. The results were obtained in a similar manner with the mal-distribution experiment. Q_{hold} is the amount of water retained in the porous media and Q_{inject} is the total amount injected from the syringes. A straightforward relation holds that $Q_{inject} = Q_{total} + Q_{hold}$; that is, the total collected water at both channels plus the hold-up water in porous media equals the injected water from the syringes. As can be seen in Fig. 10, substantial amount of water was hold in the carbon foam at low air flow rates, which is consistent with the visualization results in Section 3.1. Increased air flow could remove most of the water out, however, about 10% water was retained in porous media even the air flow rate was as high as $0.36\ \mathrm{l\ min^{-1}}$. Such water was transporting within the pore network, but not moving out. Interestingly, less water injection resulted in relatively higher water hold-up ratio, particularly at low air flow rates, which may be explained by a limited water hold-up capacity of the porous media. In other words, over the whole region of porous media and at any given time, there would be a portion of the pores holding up the water, others being hollow for air to pass. This characteristic of porous media in fuel cell channels may be significant considering that under drying condition, there retains certain amount of water in flow channels; whereas under flooding, still only a portion of pores (not all) hold water and air flow can always pass without channel blocking. Compared with the normal hollow channel design, therefore, channel with porous media inserts features a self-adjustment capacity in water management. Although water hold-up occurs in porous channel, the unique two phase flow patterns in porous channel guarantee the smooth air transport along the channel and towards the GDL, which provides a potential solution for flooding.

3.5. Pressure drop oscillation

As mentioned in Section 3.1, the pressure drop oscillation was observed in one of the three cases. In this section, the oscillation case was further studied using Fast Fourier Transform (FFT)

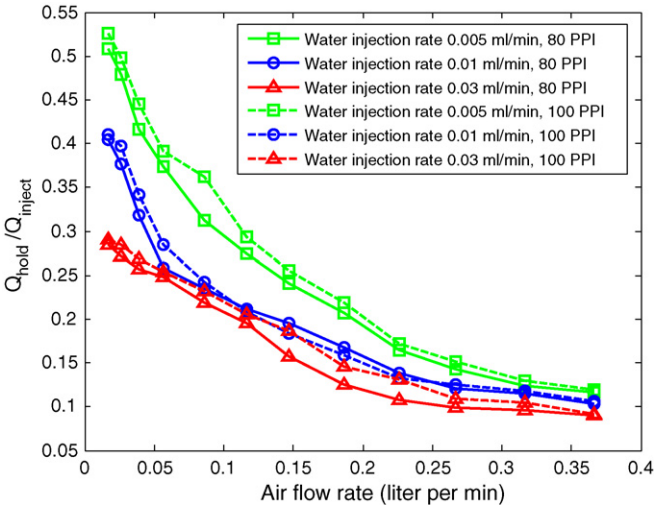

Fig. 10. The ratio of the hold-up water amount in porous media to the total injected water amount for different air flow rates and porous media pore sizes.

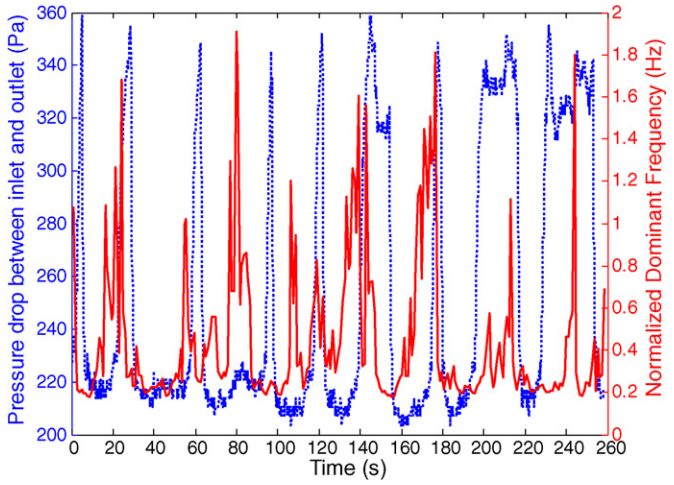

Fig. 11. The pressure drop oscillation profile and its dominant frequency plot when the air flow rate was 0.0566 l min^{-1} and water injection rate 0.01 ml min^{-1}.

technique. A co-plot of the pressure drop signal and its dominant frequency was obtain as in Fig. 11. Detailed information about the FFT algorithm for the pressure drop signal can be found in Ref. [42]. It should be noted that at a given time, the FFT was performed for a window of 40 data, with the datum corresponding to the given moment as the center of the window. Physically, the dominant frequency indicated the level of signal instability and oscillation for a given amount of data. An interesting phenomenon observed in Fig. 11 is the advances of the frequency peaks compared with the pressure drop peaks (except the last two peaks). That is to say, the pressure drop signal actually featured a highest instability right before it reached the peak; instead of a normal thinking that highest instability should occur at the peak. As explained before, when the air flow rate was 0.0566 l min^{-1}, most of the injected water was hold in various pores of the carbon foam. These water droplets were not always still in the pores, instead, they moved randomly to neighboring pores as long as sufficient pressure was supplied to overcome the capillary energy. Air flow passed though the channel via those pores without water hold-up; meanwhile, it provided the pressure build-up to move the water in pores. Every time the water droplet in one pore moved to another, pressure build-up/release cycle must accompany. As a result, the highest pressure drop instability would happen at some time during such random movement of water droplets. However, such moment may coincide with the expelling of water out of the channel at the outlet, which was indicated by the pressure drop peak. That explains why the last two dominant frequency peaks in Fig. 11 are within the peaks of pressure drop. Examining the pressure drop signal in frequency domain provides further evidence for the water transport behavior in the channel with porous media. On the other hand, the dominant frequency of pressure drop signal may be used as a novel diagnostic tool for the water transport in porous media. Pressure drop as a diagnostic tool for PEM fuel cell outputs or electrode flooding has been found in literature [43,44]. However, dominant frequency may be more advantageous due to its higher resistance to noises and sensitivity to the water behavior.

3.6. Implications for PEM fuel cell design

There are many engineering designs for the flow field in PEM fuel cell, mainstream ones including parallel, serpentine, interdigitated and pin type [45]. Although each type features its advantages, all these traditional designs are based on hollow channel concept. However, the PEM fuel cell flow channels do not have to be hollow as traditional design goes. Based on the experimental observations in this work, micro-channels with porous media (carbon foam) inserts show less severe two phase flow mal-distribution compared with hollow channels. Also, the water hold-up capacity of porous media provides a self-adjustment to the water amount in flow field, which may greatly reduce the tendency of flooding/drying during fuel cell operations. Particularly, the air flow can hardly be blocked due to the liquid water flooding in channels under the novel design of porous channel. Although the two phase pressure drop is higher than that in hollow channels, the benefits seem to be more significant. The insert of porous media into the channel does not change its original homogeneity for two phase flow. With these finding the author proposes this novel design of PEM fuel cell flow channel. Future work will include in situ performance tests of fuel cells applying this novel flow channel design.

4. Conclusions

In this study, the air–water two phase flow behavior in 1.5 mm width parallel channels with porous media inserts was experimentally investigated using a self-designed and manufactured transparent assembly. The homogeneity between the hollow channel and porous channel was verified by the negative flow resistance phenomenon at low air flow rates. By analyzing the visualization photos, three flow patterns were found under such channel configuration at increasing air flow rates: intermittent, film and chaos flows. For each pattern, the water transport/hold-up within the porous media showed different characteristics, as well as the real-time pressure drop profiles that were directly linked to water behavior. Clear pressure drop peak/bottom cycles were observed in intermittent flow case. The overall two phase flow pressure drop for porous media channels showed an approximate fourfold increase compared with hollow channels. The two phase flow mal-distribution, however, was much less severe compared with hollow channels, due to the random process of arrangement of water droplets in numerous tiny pores ($\sim$100 μm). Also, the porous media inserts featured self-adjustment capacity to water amount in flow channels, which may be significantly advantageous for water management. The air flow could thus hardly be hindered due to the flooding water when the channel had porous media inserts. Finally, the dominant frequency of pressure drop signal was found to be an effective diagnostic tool for water behavior and fuel cell performance. Findings from this study suggest that the flow channels with porous media inserts may turn out to be an effective design in handling the flow mal-distribution problem and optimizing the water management in PEM fuel cells.

Acknowledgments

Supports from Professor Yun Wang at Mechanical and Aerospace Engineering, UC Irvine are gratefully acknowledged. The author also would like to thank ERG Materials and Aerospace Corp. in providing the metal and carbon foams for this project.

References

[1] J. Larminie, A. Dicks, Fuel Cell System Explained, John Wiley & Sons, 2003, pp. 22–29.
[2] Z.H. Wang, C.-Y. Wang, K.S. Chen, J. Power Sources 94 (2001) 40–50.
[3] U. Pasaogullari, C.-Y. Wang, J. Electrochem. Soc. 151 (2004) A399–A406.
[4] X. Yu, B. Zhou, A. Sobiesiak, J. Power Sources 147 (2005) 184–195.
[5] F.Y. Zhang, X.G. Yang, C.-Y. Wang, J. Electrochem. Soc. 153 (2006) A225–A232.
[6] D. Natarajan, T.V. Nguyen, J. Electrochem. Soc. 48 (12) (2001) 1324–1335.
[7] S. Mazumder, J.V. Cole, J. Electrochem. Soc. 150 (2003) A1510–A1517.
[8] H. Meng, C.-Y. Wang, J. Electrochem. Soc. 152 (2005) A1733–A1741.
[9] Y. Wang, C.-Y. Wang, J. Electrochem. Soc. 154 (2007) B636–B643.
[10] P. Quan, B. Zhou, A. Sobiesiak, Z. Liu, J. Power Sources 152 (2005) 131–145.
[11] Y. Wang, S. Basu, C.-Y. Wang, J. Power Sources 179 (2008) 603–617.
[12] S. Maharudrayya, S. Jayanti, A.P. Deshpande, J. Power Sources 138 (2004) 1–13.

[13] S. Maharudrayya, S. Jayanti, A.P. Deshpande, J. Power Sources 144 (2005) 94–106.
[14] K. Jiao, B. Zhou, P. Quan, J. Power Sources 154 (2006) 124–137.
[15] K. Jiao, B. Zhou, P. Quan, J. Power Sources 157 (2006) 226–243.
[16] H. Masuda, K. Ito, T. Oshima, K. Sasaki, J. Power Sources 177 (2008) 303–313.
[17] I.S. Hussaini, C.-Y. Wang, J. Power Sources 187 (2009) 444–451.
[18] L. Zhang, H.T. Bi, D.P. Wilkinsona, J. Stumper, H. Wang, J. Power Sources 183 (2008) 643–650.
[19] L. Zhang, W. Du, H.T. Bi, D.P. Wilkinson, J. Stumper, H. Wang, J. Power Sources 189 (2009) 1023–1031.
[20] S. Basu, J. Li, C.-Y. Wang, J. Power Sources 187 (2009) 431–443.
[21] H. Wong, S. Morris, C.J. Radke, J. Colloid Interf. Sci. 148 (1992) 317–336.
[22] M. Chaouche, N. Rakotomalala, D. Salin, Y.C. Yortsos, Europhys. Lett. 21 (1993) 19–24.
[23] C.-Y. Wang, M. Groll, S. Rosler, C.J. Tu, Heat Recov. Syst. CHP 14 (4) (1994) 377–389.
[24] K.-K. Tio, C.Y. Liu, K.C. Toh, Heat Mass Transfer 36 (2000) 21–28.
[25] P.K. Sinha, C.-Y. Wang, Electrochim. Acta 52 (2007) 7936–7945.
[26] Y. Tabe, Y. Lee, T. Chikahisa, M. Kozakai, J. Power Sources 193 (2009) 24–31.
[27] Y. Wang, J. Power Sources 185 (2008) 261–271.
[28] J. Benziger, J. Nehlsen, D. Blackwell, T. Brennan, J. Itescu, J. Membr. Sci. 261 (2005) 98–106.
[29] B. Gao, T.S. Steenhuis, Y. Zevi, J.-Y. Parlange, R.N. Carter, T.A. Trabold, J. Power Sources 190 (2009) 493–498.
[30] K. Jiao, J. Park, X. Li, Appl. Energy (2009), doi:10.1016/j.apenergy.2009.04.041.
[31] S. Arisetty, A.K. Prasad, S.G. Advani, J. Power Sources 165 (2007) 49–57.
[32] Y. Jang, N.J. Dudney, T.N. Tiegs, J.W. Klett, J. Power Sources 161 (2006) 1392–1399.
[33] W. Yang, S. Yang, W. Sun, G. Sun, Q. Xin, J. Power Sources 160 (2006) 1420–1424.
[34] R. Ströbel, J. Garche, P.T. Moseley, L. Jörissen, G. Wolf, J. Power Sources 159 (2006) 781–801.
[35] R.W. Hornbeck, Appl. Sci. Res. 13 (1964) 224–232.
[36] A. Bhattcharya, V.V. Calmidi, R.L. Mahajan, Int. J. Heat Mass Transfer 45 (2002) 1017–1031.
[37] K.A. Triplett, S.M. Ghiaasiaan, S.I. Abdel-Khalik, D.L. Sadowski, Int. J. Multiphase Flow 25 (1999) 377–394.
[38] X.G. Yang, F.Y. Zhang, A.L. Lubawy, C.-Y. Wang, Electrochem. Solid State Lett. 7 (2004) A408–A411.
[39] M. Ozawa, K. Akagawa, T. Sakaguchi, Int. J. Multiphase Flow 15 (1989) 639–657.
[40] T. Sawai, M. Kaji, T. Kasugai, H. Nakashima, T. Mori, Exp. Therm. Fluid Sci. 28 (2004) 597–606.
[41] J.B. Kitto Jr., J.M. Robertson, Heat Transfer Eng. 10 (1) (1989) 18–25.
[42] J. Chen, B. Zhou, J. Power Sources 177 (2008) 83–95.
[43] F. Barbir, H. Gorgun, X. Wang, J. Power Sources 141 (2005) 96–101.
[44] W. He, G. Lin, T.V. Nguyen, AIChE J. 49 (12) (2003) 3221–3228.
[45] X. Li, I. Sabir, Int. J. Hydrogen Energy 30 (2005) 359–371.